MOLECULAR AND CELLULAR BIOLOGY, Dec. 2006, p. 8880–8891 Vol. 26, No. 23
0270-7306/06/$08.00+0 doi:10.1128/MCB.00751-06

Ribosomal Protein *S6* Gene Haploinsufficiency Is Associated with Activation of a p53-Dependent Checkpoint during Gastrulation▽†

Linda Panić,[1] Sanda Tamarut,[1] Melanie Sticker-Jantscheff,[2] Martina Barkić,[1] Davor Solter,[3] Miljana Uzelac,[1] Kristina Grabušić,[1] and Siniša Volarević[1]*

Department of Molecular Medicine and Biotechnology, School of Medicine, University of Rijeka, Rijeka, Croatia[1]; Institute of Cell Biology, Swiss Federal Institute of Technology (ETH), Zurich, Switzerland[2]; and Department of Developmental Biology, Max Planck Institute of Immunobiology, Freiburg, Germany[3]

Received 1 May 2006/Returned for modification 18 June 2006/Accepted 15 September 2006

Nascent ribosome biogenesis is required during cell growth. To gain insight into the importance of this process during mouse oogenesis and embryonic development, we deleted one allele of the ribosomal protein *S6* gene in growing oocytes and generated *S6*-heterozygous embryos. Oogenesis and embryonic development until embryonic day 5.5 (E5.5) were normal. However, inhibition of entry into M phase of the cell cycle and apoptosis became evident post-E5.5 and led to perigastrulation lethality. Genetic inactivation of *p53* bypassed this checkpoint and prolonged development until E12.5, when the embryos died, showing decreased expression of D-type cyclins, diminished fetal liver erythropoiesis, and placental defects. Thus, a p53-dependent checkpoint is activated during gastrulation in response to ribosome insufficiency to prevent improper execution of the developmental program.

Cell growth and division are separable processes that are intimately linked during cell proliferation (5). The molecular mechanisms of this coordination in the mammalian cell are poorly understood (20). In the presence of growth factors, nutrients, and sufficient energy levels, the cell up-regulates the synthesis of diverse macromolecules and thereby increases its size and mass (11, 14, 38, 43, 49). Deregulation of the molecular mechanisms controlling cell growth results in cells of altered size and contributes to a variety of pathological conditions, including cancer, metabolic diseases, developmental errors, and hematopoietic disorders (14, 26). It has been proposed that protein synthesis is a key determinant of cell growth (36, 40, 46). To meet the increased demand for proteins during processes that require growth, such as proliferation, differentiation, and development, the cell must increase translational capacity by up-regulating ribosome biogenesis (40, 46). Genes that control ribosome biogenesis and protein translation have been identified in *Saccharomyces cerevisiae* as critical regulators of cell growth and cell size (19, 20, 53). Ribosome biogenesis is the most energy-consuming process in cell proliferation, and alterations in this process can lead to quantitative or qualitative defects in protein translation, which could have deleterious consequences on the cell (41).

There is a large amount of nascent ribosome synthesis during the growth phase of the developing mouse oocyte (24). Since maternally inherited ribosomes are rapidly exhausted during the first three cleavages, nascent ribosome biogenesis is activated in the six- to eight-cell-stage embryo (22). After a relatively silent period of ribosome biogenesis in the blastocyst, this process is again dramatically up-regulated during gastrulation, which is associated with the start of a huge increase in the rate of proliferation and differentiation (33). It could be anticipated that an error in ribosome biogenesis would have pronounced effects on these three developmental periods through impaired protein translation (22, 24, 33).

We hypothesized that a defect in ribosome biogenesis could negatively affect oogenesis and embryonic development not only through impaired translation of specific mRNAs but also via activation of a checkpoint regulatory mechanism (10, 13, 37, 41, 44, 48, 56).

In order to gain insight into the processes which govern ribosomal biogenesis during oogenesis and embryogenesis, we conditionally inactivated one allele of the ribosomal protein *S6* gene in growing oocytes and generated *S6*-heterozygous embryos. We show that *S6* gene haploinsufficiency is associated with the activation of a p53-dependent checkpoint during gastrulation. Genetic inactivation of p53 bypassed this checkpoint and prolonged development of *S6*-heterozygous embryos until embryonic day 12.5 (E12.5), when they died with decreased expression of D-type cyclins, greatly diminished fetal liver erythropoiesis, and placental defects.

MATERIALS AND METHODS

Mice and embryo collection. *Zp3-Cre*, $S6^{lox/lox}$, and $Arf^{-/-}$ mice have previously been generated (8, 48, 55). *Sox2-Cre*, $p53^{-/-}$, and $p21^{-/-}$ mice were purchased from the Jackson Laboratory (4, 12, 17). All mice were kept on the C57BL/6 genetic background. Embryo collection and preparation were performed as described previously (31). Briefly, noon on the day of the vaginal plug was taken as day 0.5 of gestation (E0.5). Pregnant females were sacrificed at different time points of gestation, and postimplantation embryos were separated from maternal tissue under a dissecting microscope (Stereomicroscope SZX 12; Olympus) in Dulbecco's modified Eagle's medium (DMEM) containing 25 mM HEPES (pH 7.4) and 10% fetal bovine serum by using fine forceps. Genotyping of embryos and mice was performed by PCR analysis using specific primers (4, 17, 44, 55). All procedures with mice were conducted with the approval of the ethical committee of the School of Medicine, University of Rijeka, in accordance with relevant guidelines and regulations.

* Corresponding author. Mailing address: Department of Molecular Medicine and Biotechnology, School of Medicine, University of Rijeka, Braće Branchetta 20, 51000, Rijeka, Croatia. Phone: 385-51 651 120. Fax: 385-51 651 197. E-mail: vsinisa@medri.hr.

† Supplemental material for this article may be found at http://mcb.asm.org/.

▽ Published ahead of print on 25 September 2006.

Histological analysis and immunohistochemistry. Embryos and ovaries were fixed overnight in 10% formalin and embedded in paraffin. Sections 4 μm thick were cut and stained with hematoxylin and eosin (H&E). For immunohistochemistry, anti-p53 (Novocastra Laboratories), anti-phospho-ATM/ATR substrate (Cell Signaling Technology), and anti-phospho-Ser139-histone H2A.X (Cell Signaling Technology) primary antibodies were used. Biotinylated anti-rabbit antibody was used as the secondary antibody, and detection was done by using an ABC system with diaminobenzidine substrate (Vector Lab).

Detection of BrdU-labeled and apoptotic cells. 5-Bromo-2′-deoxyuridine (5-BrdU) (100 μg/gram of body weight) was injected intraperitoneally into pregnant females (Sigma-Aldrich Chemie GmbH). The females were sacrificed 1 h after injection, and deciduas were processed for immunohistochemistry. 5-BrdU-positive cells were detected using a BrdU in situ detection kit (BD Biosciences Pharmingen). Apoptotic cells were identified by immunohistochemistry using antibody against activated caspase-3 (Cell Signaling Technology). BrdU-positive cells and apoptotic cells were counted on serial sections, and the number was compared to the total number of cells.

Detection of mitotic cells. Mitotic cells were counted on H&E-stained histological sections of embryos, and the number was compared to the total number of cells.

Blastocyst outgrowth. E3.5 embryos (blastocysts) were flushed from uterine horns with DMEM plus 10% serum and 25 mM HEPES (pH 7.4) and cultured individually on gelatinized plates at 37°C in 5% CO_2 in ES-DMEM without leukemia inhibitory factor (31). After five days in culture, embryos were analyzed by phase-contrast microscopy (IX 71; Olympus) and scraped, and their genotype was determined by PCR.

RNA isolation and Northern blot analysis. Total RNA was extracted from E9.5 embryos using TRIzol (Invitrogen Life Technologies). RNA was separated on 1% agarose/formaldehyde gel and transferred to Hybond N^+ membrane (Amersham Biosciences), hybridized at 52°C with cDNA probes labeled, and detected with an AlkPhosDirect Kit (Amersham Biosciences).

Analysis of rRNA processing. Mouse embryonic fibroblasts (MEFs) were starved for 30 min in methionine-free medium, incubated for 30 min with 25 μCi/ml L-[methyl-^{3}H]methionine (Amersham Biosciences), and then chased in medium containing nonradioactive methionine for 5 min. Total RNA, isolated from the same number of cells, was separated on a formaldehyde-agarose gel and blotted to the Hybond N^+ membrane, which was dried and treated with EN^{3}HANCE (New England Nuclear) and exposed to Kodak BioMax MS film (Sigma).

rRNA processing in embryos was analyzed by Northern blotting using a specific 5′ external transcribed sequence (5′ETS) rRNA probe. The 5′ETS probe was generated by PCR of genomic DNA by using the following primers: 5′-TC CAAGTGTTCATGCCACGTGCCTC-3′ (forward) and 5′-ACAAGAAACAG CGCGTGCACACACC-3′ (reverse). Northern blotting was performed as described above, except that the membrane was hybridized at 45°C.

CFSE labeling. Cell division of serum-stimulated MEFs was analyzed using 5 μM 5-6-carboxyfluorescein diacetate succinimidyl ester (CFSE) labeling (Molecular Probes). This method is based on the approximately twofold decreases in CFSE fluorescence after each cell division (29). Briefly, MEFs (10^6/ml of phosphate-buffered saline) were incubated with CFSE at 37°C for 10 min in CO_2 incubator, washed twice with 2% fetal calf serum (FCS) in phosphate-buffered saline, plated, and stimulated with 10% FCS in DMEM for 96 h. CFSE intensity was analyzed by flow cytometry on FACScan (Becton Dickinson) using Cell Quest software. Ten thousand events were collected.

Immunoblotting. Embryo lysates were prepared with radioimmunoprecipitation assay buffer (44). Fifty micrograms of total proteins was electrophoresed on polyacrylamide gels. Western blots were probed with antibodies against the following proteins: actin, Cdk4 (Chemicon International), cyclin D1, cyclin D3, cyclin E, Cyclin A, Cdk2, P-RB-S780 (all from Santa Cruz Biotechnology), retinoblastoma protein (RB) (BD Pharmingen), P-RB-T821 (Abcam), ribosomal protein S6 (a kind gift from George Thomas and Stefano Fumagalli), and L11 (produced by immunization of rabbits with a synthetic peptide, corresponding to amino acid residues 150 to 169). Primary antibodies were detected by using horseradish peroxidase-conjugated antibodies (Santa Cruz Biotechnology) and an ECL kit (Amersham Biosciences).

In vitro hematopoietic colony assays. Fetal livers were collected from E12.5 embryos, and single-cell suspensions were prepared. An aliquot was counted to determine the nucleated cell number. In each 35-mm dish, 2×10^4 cells were plated in triplicate in methylcellulose medium containing 50 ng/ml stem cell factor, 10 ng/ml interleukin 3 (IL-3), 10 ng/ml IL-6, and 3 U/ml erythropoietin (MethoCult M3434; Stem Cell Technologies). BFU-E (burst-forming units-erythroid) colonies were counted after 9 days (23).

Flow cytometry. Single cell suspensions from fetal livers were washed in Iscove's modified Dulbecco's medium (Stem Cell Technologies) containing 2% FCS at 4°C, and 1×10^6 cells were stained with monoclonal antibodies to c-kit and Ter-119 (both from Pharmingen). Flow cytometry was performed with a FACScan (Becton Dickinson) using Cell Quest software. Ten thousand events were collected.

Quantitative RT-PCR. Total RNA was extracted and purified from embryos using TRIzol reagent (Invitrogen Life Technologies). One μg of total RNA was reverse transcribed to cDNA with random hexamers using a SuperScript III first-strand synthesis system for real-time PCR (RT-PCR) (Invitrogen Life Technologies). For the quantitative RT-PCRs, cDNA was diluted 1:120 and amplified using a LightCycler (Roche) and a LightCycler FastStart DNA Master SYBR Green I kit (Roche) with the following primers: for cyclin D1, 5′-CTGACACC AATCTCCTCAACG-3′ (forward) and 5′-GCCAGGTTCCACTTGAGC-3′ (reverse); for cyclin D3, 5′-AAAGGAGATCAAGCCGCACAT-3′ (forward) and 5′-GTTCATAGCCAGAGGGAAGACATC-3′ (reverse). For internal control we used the following primers for actin: 5′-TTCCTATGTGGGCGACGA GG-3′ (forward) and 5′-CTCCTTAATGTCACGCACGATTTC-3′ (reverse). The relative quantification of gene expression was calculated as described by the manufacturer.

RESULTS

Specific deletion of the *S6* gene in oocytes and generation of *S6*-heterozygous embryos. One *S6* allele was specifically deleted in growing oocytes of $S6^{wt/lox}$ females by activation of a zona pellucida 3-Cre (*Zp3-Cre*) transgene (8, 48). These females were bred with wild-type males, and the genotype of their progeny was determined. If deletion of the $S6^{lox}$ allele was complete, two categories of progeny, $S6^{wt/wt}$ and $S6^{wt/del}$, could be expected in a 1:1 ratio. In contrast to expectations, PCR analysis revealed the presence of $S6^{wt/wt}$ mice only (Fig. 1A), indicating that deletion of one *S6* allele is incompatible with complete embryonic development.

To determine the effect of disrupting the *S6* gene on the growth and differentiation of primary oocytes, ovaries from $S6^{lox/lox}$/*Zp3-Cre*$^+$, $S6^{wt/lox}$/*Zp3-Cre*$^-$ and $S6^{wt/lox}$/*Zp3-Cre*$^+$ mice were subjected to histological analyses. In $S6^{lox/lox}$/*Zp3-Cre*$^+$ ovaries, primordial follicles were present, but there was a complete absence of secondary and tertiary follicles, demonstrating that the conditional deletion of both *S6* alleles prevents cell growth in this model. In contrast, in ovaries from $S6^{wt/lox}$/*Zp3-Cre*$^+$ mice, follicles were seen at various stages of development, ranging from primordial to fully developed (see Fig. S1 in the supplemental material). These results suggest that requirements for ribosomes are less stringent during mouse oogenesis than previously thought (24). In contrast to these results, a half dosage of some ribosomal proteins in *Drosophila* sp. reduces female fertility (25).

To assess if $S6^{wt/lox}$/*Zp3-Cre*$^+$ oocytes differentiated into fertilization-competent egg cells and to determine the consequence of deletion of one *S6* allele on embryonic development, the number of embryos and their morphology were analyzed at different days of gestation (31) (Fig. 1B). No significant morphological differences between mutant and wild-type E5.5 embryos were observed. Approximately half of the E6.5 embryos were smaller than the others, and all of these were $S6^{wt/del}$ mutants. Mutant E7.5 embryos were also smaller than their wild-type counterparts and did not appear to progress significantly beyond E6.5. The expected 1:1 ratio of $S6^{wt/wt}$ to $S6^{wt/del}$ embryos was observed until E7.5. At E8.5, wild-type embryos developed past the gastrulation stage with a distinct anterior-posterior pattern, whereas all E8.5 mutant embryos were

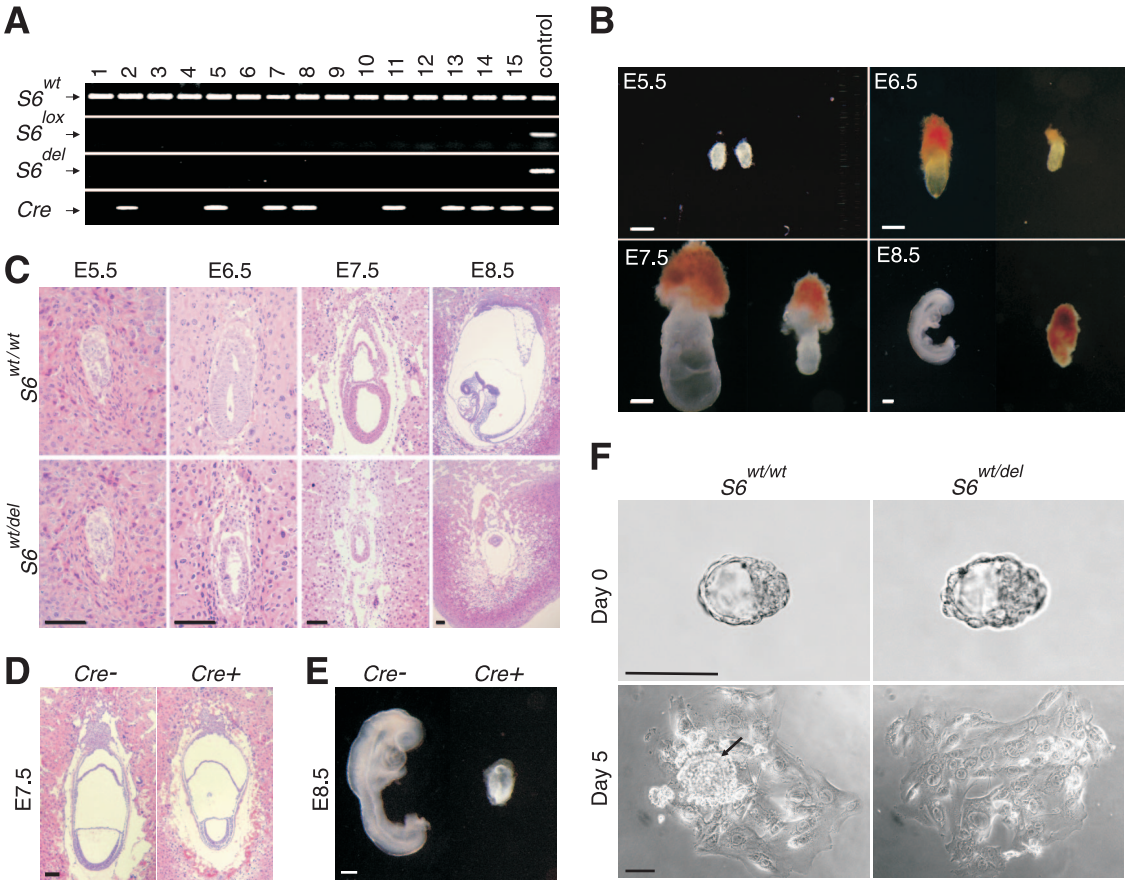

FIG. 1. Generation and phenotypic characterization of *S6*-heterozygous embryos. (A) PCR analysis of representative tail tip DNAs of pups from intercrosses of $S6^{wt/lox}$/*Zp3-Cre*$^{+}$ females and wild-type males ($n = 128$). (B) Morphology of representative $S6^{wt/wt}$ and $S6^{wt/del}$ embryos at the indicated stages of gestation. (C) H&E staining of histological sections of $S6^{wt/wt}$ and $S6^{wt/del}$ embryos at the indicated stages. (D) Histological sections of E7.5 $S6^{wt/lox}$/*Sox2-Cre*$^{-}$ and $S6^{wt/lox}$/*Sox2-Cre*$^{+}$ embryos were stained with H&E. (E) Morphology of representative E8.5 $S6^{wt/lox}$/*Sox2-Cre*$^{-}$ ($n = 32$) and $S6^{wt/lox}$/*Sox2-Cre*$^{+}$ ($n = 41$) embryos. (F) Defective inner cell mass (arrow) in $S6^{wt/del}$ embryo outgrowths. $S6^{wt/wt}$ and $S6^{wt/del}$ embryos derived from blastocyst outgrowths after 5 days in culture in the absence of leukemia inhibitory factor. Embryos shown in panels B, E, and F were genotyped by PCR analysis. Scale bars, 100 μm (C, D, and F) and 200 μm (B and E).

in resorption (Fig. 1B; see Table S1 in the supplemental material).

***S6*-heterozygous embryos die during gastrulation.** The time of apparent developmental failure of $S6^{wt/del}$ embryos coincides with gastrulation. During this developmental period, dramatic increases in the rate of cell proliferation are followed by the establishment of the three primary germ layers (33). To understand the developmental defect of $S6^{wt/del}$ embryos in greater detail, we compared H&E-stained histological sections of $S6^{wt/wt}$ and $S6^{wt/del}$ E5.5, E6.5, E7.5, and E8.5 embryos (31) (Fig. 1C). Both mutant and control E5.5 embryos displayed the characteristic elongated egg cylinder. Wild-type E6.5 embryos showed a clear morphological distinction between the embryonic and extraembryonic ectoderm and between the embryonic and extraembryonic endoderm (Fig. 1C). In contrast, E6.5 mutant embryos exhibited a reduced and disorganized embryonic and extraembryonic region. Additionally, a change in the shape of the cells was observed (Fig. 1C). Wild-type E7.5 embryos increased in size and further progressed in their development, while mutant embryos did not. By E8.5, all $S6^{wt/del}$ embryos were being resorbed (Fig. 1C).

Extraembryonic tissue allows embryos to attach to the uterus during implantation, conveys nutrients to the embryo, removes its waste products, and later participates in the formation of the placenta. To determine its contribution to the mutant phenotype in vivo, we crossed $S6^{lox/lox}$ females with *Sox2-Cre* males to specifically delete one *S6* allele in the epiblast at early gastrulation stages (12). Growth of the embryonic but not extraembryonic region was inhibited in E7.5 $S6^{wt/lox}$/*Sox2-Cre*$^{+}$ embryos (Fig. 1D). As a consequence, $S6^{wt/lox}$/*Sox2-Cre*$^{+}$ embryos died by E8.5, indicating that the mutant phenotype could not be rescued with wild-type extraembryonic tissue (Fig. 1E). A PCR analysis of DNA isolated $S6^{wt/lox}$/*Sox2-Cre*$^{+}$ embryos showed that one *S6* allele is deleted in the embryonic but not extraembryonic region (data not shown). To assess if $S6^{wt/del}$ embryos will manifest any pathology when grown in culture, where rates of cell division are slower (13), E3.5 blastocysts obtained from crosses between $S6^{wt/lox}$/*Zp3-Cre*$^{+}$ females and wild-type males were isolated and individually cultured in vitro (31) (Fig. 1F). Sixty-nine out of seventy-four blastocysts attached to the plate after three days in culture. After five days in culture, the inner cell mass, which contributes to formation

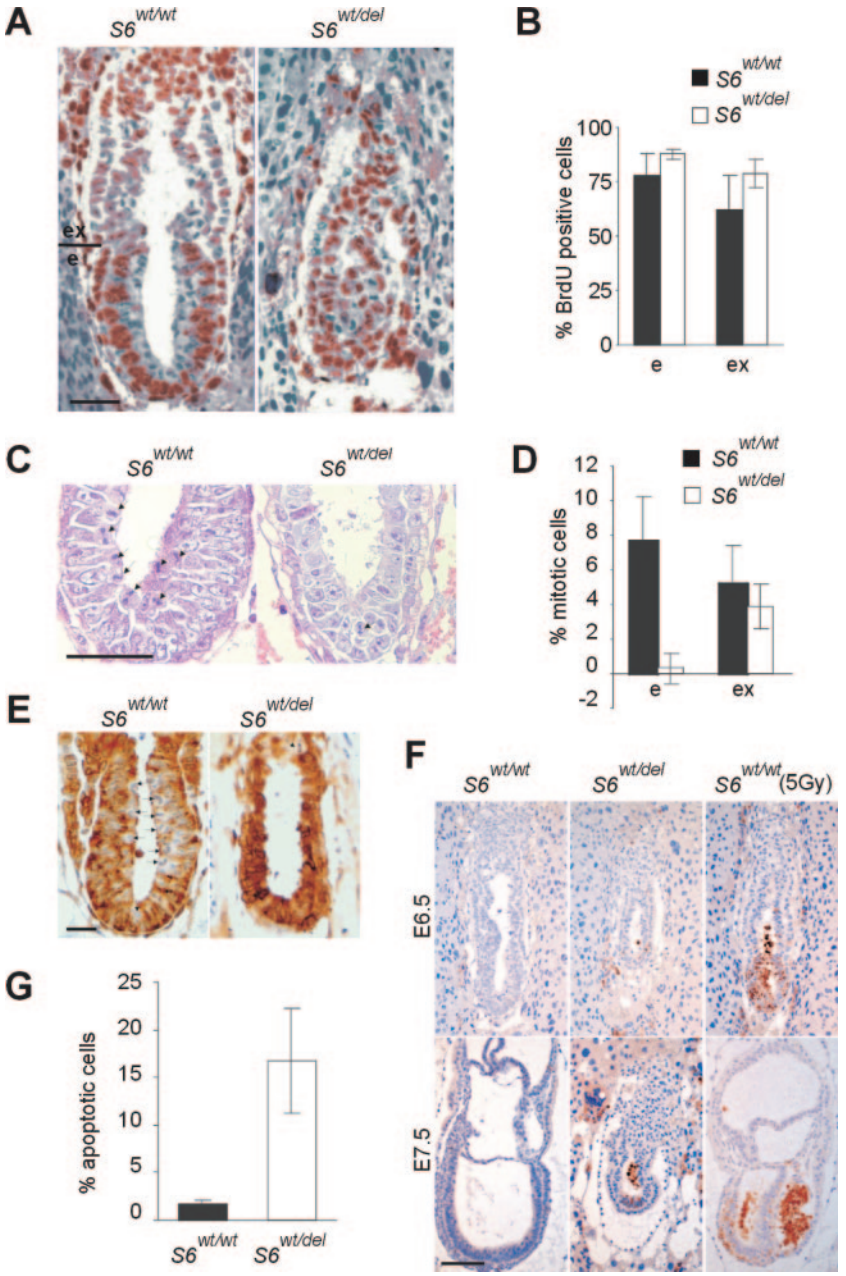

FIG. 2. Impaired cellular proliferation and increased apoptosis in $S6^{wt/del}$ embryos. (A) 5-BrdU-labeled cells (brown) in sections of E6.5 $S6^{wt/wt}$ and $S6^{wt/del}$ embryos. (B) Percentage of cells that were BrdU labeled in embryonic and extraembryonic regions of E6.5 $S6^{wt/wt}$ ($n = 15$) and $S6^{wt/del}$ ($n = 13$) embryos. (C) Mitotic figures in sections of E6.5 $S6^{wt/wt}$ and $S6^{wt/del}$ embryonic regions are indicated by arrows. (D) Percentage of cells that were in mitosis in embryonic and extraembryonic regions of E6.5 $S6^{wt/wt}$ ($n = 12$) and $S6^{wt/del}$ ($n = 13$) embryos. (E) Immunohistochemistry of sections of E6.5 $S6^{wt/wt}$ and $S6^{wt/del}$ embryos with antibodies against phosphorylated Tyr-15-Cdk1. (F) Apoptosis in sections of E6.5 and E7.5 $S6^{wt/wt}$ and $S6^{wt/del}$ embryos. Gamma irradiation (5Gy) induced massive apoptosis in the embryonic part of E6.5 and E7.5 $S6^{wt/wt}$ embryos. (G) Percentages of apoptotic cells in E7.5 $S6^{wt/wt}$ ($n = 12$) and $S6^{wt/del}$ ($n = 10$) embryos. e and ex in panels A, B, and D indicate embryonic and extraembryonic regions, respectively. Scale bars, 50 μm (A, C, and E) and 100 μm (F). Error bars in panels B, D, and G denote standard deviations (SD).

of the embryo, was absent in 100% of $S6^{wt/del}$ embryo outgrowths ($n = 29$) and only 22.5% of control embryos ($n = 40$) (Fig. 1F). In contrast, $S6^{wt/del}$ mutation did not affect giant trophoblast cells that contribute to the development of the extraembryonic tissue (Fig. 1F). These results suggest that the phenotype of $S6^{wt/del}$ embryos is not merely a consequence of extremely fast cell division during gastrulation in vivo (33).

Proliferative defect and increased apoptosis of *S6*-heterozygous embryonic cells at gastrulation. To determine if developmental failure of $S6^{wt/del}$ embryos is caused by perturbation

of the cell cycle, we measured the incorporation of 5-BrdU into DNA of E6.5 mutant and control embryos in vivo (13). The percentages of 5-BrdU-labeled cells were similar in mutant and control embryos (Fig. 2A and B), indicating that G_1/S transition in $S6^{wt/del}$ E6.5 embryos is not impaired. Surprisingly, the percentage of mitotic figures was dramatically decreased in the embryonic region but only slightly decreased in the extraembryonic regions of $S6^{wt/del}$ embryos (Fig. 2C and D), suggesting that E6.5 $S6^{wt/del}$ embryonic cells failed to enter mitosis (21). The dephosphorylation of Tyr15-Cdk1 is associated with the G_2/M transition. E6.5 $S6^{wt/wt}$ mitotic cells weakly stained for phosphorylated Tyr-15-Cdk1, while the remaining cells strongly stained. In contrast, all $S6^{wt/del}$ embryonic cells, except rare mitotic cells, stained for phosphorylated Tyr15-Cdk1 (Fig. 2E). In addition, there was no difference in staining with anti-Cdk1 antibodies between mutant and control embryos (data not shown). These results suggest that the deletion of one *S6* allele prevents cells from entering the M phase by inhibiting dephosphorylation and activation of Cdk1, although we do not have any direct evidence for a causal relationship between these two events. Together, these results could largely explain the phenotype of $S6^{wt/del}$ embryos.

To find out if programmed cell death contributes to the mutant phenotype, we tested the expression of the activated form of caspase-3 in tissue sections of mutant and control E6.5 and E7.5 embryos (Fig. 2F). We observed only a few apoptotic cells in $S6^{wt/wt}$ embryos. A slightly higher number of apoptotic cells were observed with E6.5 $S6^{wt/del}$ embryos. Around 17% of cells in E7.5 $S6^{wt/del}$ embryos were apoptotic, and they were confined to the embryonic region (Fig. 2G). Similar results were observed by using TdT-mediated dUTP nick end labeling (data not shown). These results indicate that increased apoptosis also contributes to the phenotype of $S6^{wt/del}$ embryos. Furthermore, cell death that is the result of a permanent cell cycle block could also contribute to the lethality of these embryos.

***S6* heterozygosity triggers a p53-dependent checkpoint during gastrulation.** There are at least two models that could explain the phenotype of $S6^{wt/del}$ embryos. One is that a reduced level of S6 is rate limiting for ribosome biogenesis and may constitute a bottleneck for protein synthesis in highly proliferative cells at gastrulation (33). The other possibility is that the embryonic cells possess molecular mechanisms that sense an error in ribosome biogenesis at the onset of gastrulation and eliminate potentially defective cells (10, 13). A number of different stresses activate the tumor suppressor p53 (47). We hypothesized that a defect in a component of the 40S ribosome could also trigger this stress response. We first compared the protein expression of p53 in $S6^{wt/wt}$ and $S6^{wt/del}$ embryos. No staining was observed in $S6^{wt/wt}$ E6.5 embryos, while the majority of $S6^{wt/del}$ cells strongly stained with anti-p53 antibodies (Fig. 3A).

To address if p53 is responsible for the phenotype of $S6^{wt/del}$ embryos, the $S6^{wt/del}$ mutation was introduced into the *p53*-null background by appropriate breeding (16). Since $S6^{wt/del}/p53^{-/-}$ pups were not found at birth, we examined $S6^{wt/del}/p53^{-/-}$ embryos at different stages of gestation. At E7.5, they were larger than $S6^{wt/del}$ and smaller than $S6^{wt/wt}/p53^{-/-}$ embryos (Fig. 3B). The inactivation of *p53* overcomes the cell cycle block and apoptosis in E7.5 $S6^{wt/del}$ embryos (17, 47) (Fig. 3C and D). Strikingly, $S6^{wt/del}/p53^{-/-}$ embryos developed past the gastrulation stage, even though they were smaller than their $S6^{wt/wt}/p53^{-/-}$ littermates (Fig. 3E). These results demonstrate that lethality in $S6^{wt/del}$ embryos is the result of p53-dependent checkpoint activation at gastrulation. They also suggest that the smaller size of $S6^{wt/del}/p53^{-/-}$ embryos could be the result of decreased translational capacity. However, we do not have direct experimental evidence to support that possibility.

Impaired translation of mRNAs encoding key DNA damage repair or replication proteins could lead to DNA damage and the induction of p53 in $S6^{wt/del}$ embryos (47). Histological sections of these embryos did not stain positive with antibodies against the ATM/ATR phosphorylated consensus sequence or histone H2A.X phosphorylated on Ser139, suggesting that the DNA damage is not responsible for the induction of p53 in *S6*-deficient embryonic cells (2) (Fig. 3F).

Next, we wanted to elucidate the molecular mechanisms that increase p53 levels in S6-deficient embryonic cells. The nucleolar protein p19Arf regulates p53 levels under stress conditions (reviewed in reference 28). We speculated that, upon perturbations in ribosome biogenesis in $S6^{wt/del}$ embryonic cells, p19Arf becomes accessible to bind and antagonize Mdm2 function and activate p53. Interestingly, genetic inactivation of *p19Arf* did not rescue the lethality of *S6*-heterozygous embryos at gastrulation, suggesting that p19Arf is not required for this checkpoint response (55) (Fig. 3G).

We set out to determine molecules that may function downstream of p53 in this checkpoint regulatory pathway. A candidate gene is the cell cycle inhibitor $p21^{CIP1}$, a transcriptional target of the p53 tumor suppressor. Therefore, we genetically inactivated $p21^{CIP1}$ in $S6^{wt/del}$ embryos (4). $S6^{wt/del}/p21^{CIP1-/-}$ embryos were significantly smaller and more developmentally retarded than $S6^{wt/del}/p53^{-/-}$ embryos at E8.5 and E9.5 (Fig. 3H), indicating that $p21^{CIP1}$ only partially accounts for the effect of p53 in $S6^{wt/del}$ embryos during gastrulation, probably because p53 can still induce apoptosis as well as inhibit ribosome biogenesis.

Ribosome biogenesis defect in $S6^{wt/del}/p53^{-/-}$ embryos. To gain insight into the postgastrulation development of $S6^{wt/del}/p53^{-/-}$ embryos, we analyzed their number and morphology at different stages. These embryos were detected at the expected Mendelian distribution until E10.5, about half of them were still viable at E12.5, but no live mutant embryos were observed at E13.5 (see Table S2 in the supplemental material). $S6^{wt/del}/p53^{-/-}$ embryos were smaller than their $S6^{wt/wt}/p53^{-/-}$ littermates from gastrulation to E12.5 (Fig. 3B and E and data not shown).

To understand how the $S6^{wt/del}$ mutant genotype is responsible for the phenotype of $S6^{wt/del}/p53^{-/-}$ embryos, we first determined the level of S6 protein. S6 was significantly decreased, but there was no effect on L11 ribosomal protein (Fig. 4A). A Northern blot analysis of total RNA isolated from E10.5 $S6^{wt/del}/p53^{-/-}$ embryos employing 5′ETS, ITS-1 (internal transcribed sequence 1), and 18S rRNA specific probes revealed that they accumulated 34S rRNA precursor, suggesting an rRNA processing defect (Fig. 4B and data not shown). The same rRNA precursor also accumulated in E12.5 $S6^{wt/del}/p53^{-/-}$ embryos (Fig. 4B and data not shown) as well as in *S6*-deficient livers and T cells (44, 48). Most likely, as a con-

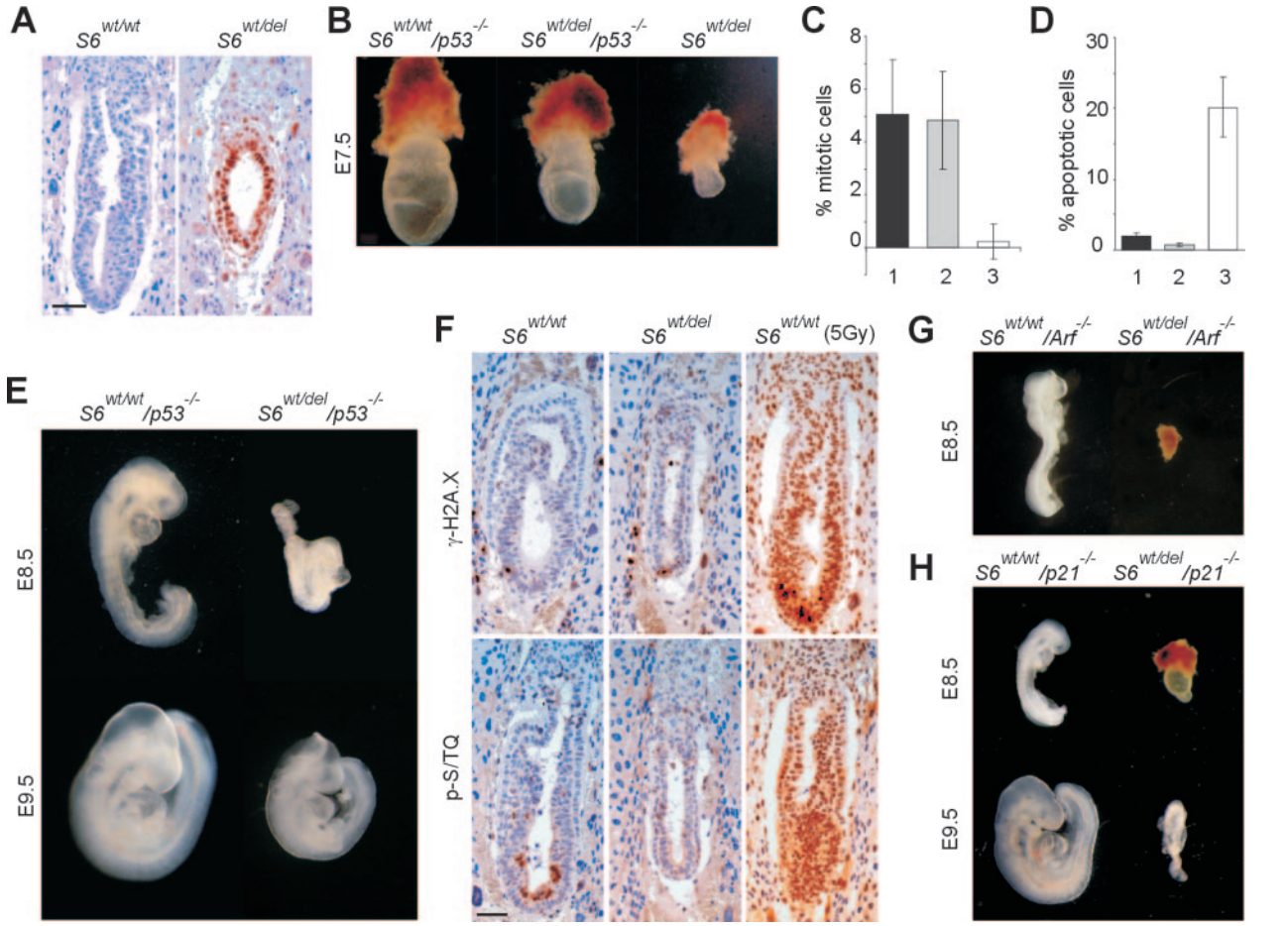

FIG. 3. A p53-dependent checkpoint is activated in *S6*-heterozygous embryos. (A) Immunohistochemistry of sections of E6.5 $S6^{wt/wt}$ and $S6^{wt/del}$ embryos with antibodies against p53. (B) Morphology of representative E7.5 $S6^{wt/wt}/p53^{-/-}$, $S6^{wt/del}/p53^{-/-}$, and $S6^{wt/del}$ embryos. (C) Percentage of mitotic cells in the embryonic region of E7.5 $S6^{wt/wt}/p53^{-/-}$ ($n = 8$), $S6^{wt/del}/p53^{-/-}$ ($n = 8$), and $S6^{wt/del}$ ($n = 7$) embryos. (D) Percentage of apoptotic cells in E7.5 $S6^{wt/wt}/p53^{-/-}$ ($n = 8$), $S6^{wt/del}/p53^{-/-}$ ($n = 7$), and $S6^{wt/del}$ ($n = 8$) embryos. $S6^{wt/wt}/p53^{-/-}$, $S6^{wt/del}/p53^{-/-}$, and $S6^{wt/del}$ genotypes in C and D are indicated with 1, 2, and 3, respectively. (E) Whole-mount preparations of representative E8.5 and E9.5 $S6^{wt/wt}/p53^{-/-}$ and $S6^{wt/del}/p53^{-/-}$ embryos. (F) Immunohistochemistry of sections of E6.5 $S6^{wt/wt}$ and $S6^{wt/del}$ embryos with antibodies against the ATM/ATR phosphorylated consensus sequence (p-S/TQ) and phosphohistone H2A.X (γ-H2A.X). The majority of cells from E6.5 $S6^{wt/wt}$ embryos stained strongly positive with these antibodies 30 min after gamma irradiation (5Gy). (G) Morphology of representative $S6^{wt/wt}/p19Arf^{-/-}$ ($n = 14$) and $S6^{wt/del}/p19Arf^{-/-}$ ($n = 11$) embryos at E8.5. (H) Morphology of representative $S6^{wt/wt}/p21^{-/-}$ and $S6^{wt/del}/p21^{-/-}$ embryos at E8.5 and E9.5. Scale bar, 50 μm (A and F). Error bars in panels C and D denote SD. Embryos in panels B, E, G, and H were genotyped by PCR analysis.

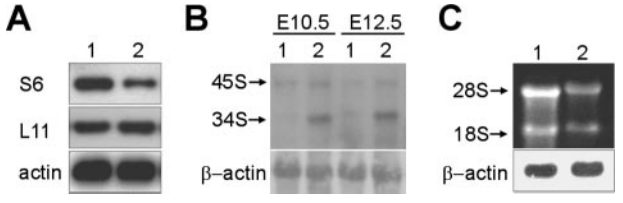

FIG. 4. Defective ribosome biogenesis in $S6^{wt/del}/p53^{-/-}$ embryos. (A) Western blot of E10.5 embryo lysates with antibodies against ribosomal proteins S6, L11, and actin. (B) Northern blot analysis of total RNA isolated from E10.5 and E12.5 embryos using 5′ETS specific probe. Positions of 45S rRNA and 34S rRNA are indicated. (C) Ethidium bromide staining of RNA from E10.5 embryos. Positions of 18S and 28S rRNAs in the gel are indicated. RNA loading in panels B and C was normalized to the expression of β-*actin* mRNA determined by Northern blotting. $S6^{wt/wt}/p53^{-/-}$ and $S6^{wt/del}/p53^{-/-}$ genotypes in panels A to C are indicated with 1 and 2, respectively.

sequence of this processing defect, the amounts of 18S and 28S rRNAs were significantly decreased in $S6^{wt/del}/p53^{-/-}$ embryos, suggesting a serious deficiency in the amount of 40S and 60S ribosomal subunits, respectively (Fig. 4C).

Phenotypes of $S6^{wt/del}/p53^{-/-}$ MEFs. Pulse-chase labeling experiments revealed that $S6^{wt/del}/p53^{-/-}$ E12.5 MEFs also accumulated 34S rRNA precursor (Fig. 5A). In order to determine if developmental failure of $S6^{wt/del}/p53^{-/-}$ embryos is a consequence of defects in cellular proliferation, we first analyzed this process in E12.5 $S6^{wt/wt}/p53^{-/-}$ and $S6^{wt/del}/p53^{-/-}$ MEFs. Surprisingly, despite a defect in rRNA processing in $S6^{wt/del}/p53^{-/-}$ MEFs, expression of D-type cyclins and proliferation were comparable to those of the control (Fig. 5B and C; see Fig. S3 in the supplemental material). Furthermore, the cell size of $S6^{wt/del}/p53^{-/-}$ MEFs was indistinguishable from that of their $S6^{wt/wt}/p53^{-/-}$ counterparts (Fig. 5D). These results suggest that a defect in ribosome biogenesis in $S6^{wt/del}$

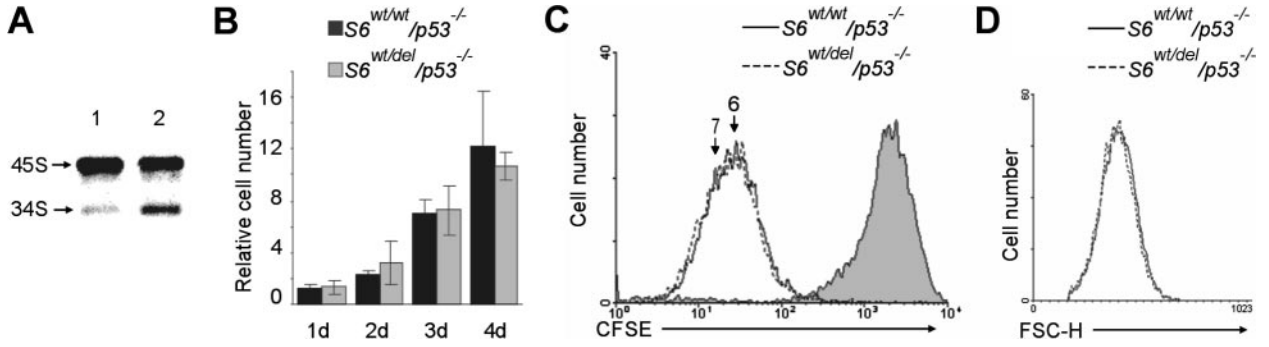

FIG. 5. Characterization of $S6^{wt/del}/p53^{-/-}$ MEFs. (A) E12.5 MEFs were pulse-chase labeled with L-[methyl-^{3}H]methionine. $S6^{wt/wt}/p53^{-/-}$ and $S6^{wt/del}/p53^{-/-}$ genotypes are indicated with 1 and 2, respectively. Positions of major rRNA precursors are indicated. RNA loading was normalized to equal the cell number. The experiment is representative of four independent experiments. (B) Relative number of asynchronously proliferating $S6^{wt/wt}/p53^{-/-}$ and $S6^{wt/del}/p53^{-/-}$ MEFs at the indicated times were calculated from the results of three independent experiments. (C) Division of CFSE-labeled $S6^{wt/wt}/p53^{-/-}$ and $S6^{wt/del}/p53^{-/-}$ MEFs. The filled area represents CFSE labeling of MEFs before they divided for the first time. The number of cell divisions is indicated above the peaks. Data are representative of four independent experiments. (D) The cell size of proliferating E12.5 $S6^{wt/wt}/p53^{-/-}$ and $S6^{wt/del}/p53^{-/-}$ MEFs was measured by forward light scatter (FSC-H) using a flow cytometer. Error bars in panel B denote SD.

MEFs in the absence of p53 does not compromise cell cycle progression and cell growth per se. However, these results do not rule out the possibility that $S6^{wt/del}/p53^{-/-}$ cells exhibit some defects in these responses in vivo.

Phenotypes of $S6^{wt/del}/p53^{-/-}$ embryos. To determine if the phenotype of $S6^{wt/del}/p53^{-/-}$ embryos is a consequence of defects in cellular proliferation, we analyzed this process in $S6^{wt/wt}/p53^{-/-}$ and $S6^{wt/del}/p53^{-/-}$ embryos. Analyses of cell cycle regulators in E10.5 $S6^{wt/del}/p53^{-/-}$ embryos revealed that the protein levels of cyclin D1 and cyclin D3 were decreased (Fig. 6A). In contrast, the expression of cyclin E, cyclin A, Cdk2, and Cdk4 was unaltered (Fig. 6A). Quantitative RT-PCR analysis revealed that cyclin D1 and cyclin D3 mRNA levels are comparable in mutant and control embryos (Fig. 6B). The data suggest a posttranscriptional defect in the expression of D-type cyclins, most likely at the level of translation. RB was hypophosphorylated in vivo on Ser780, a residue thought to be specific for D-type cyclin-dependent Cdks, probably as a result of lower levels of D-type cyclins. In contrast, the phosphorylation of RB on cyclin E- and A-specific RB residue, Thr821, was unaltered (Fig. 6A). Despite defects in cyclin D-dependent RB phosphorylation, we found that the incorporation of BrdU in most tissues of E11.5 $S6^{wt/del}/p53^{-/-}$ embryos was only slightly decreased in comparison to their $S6^{wt/wt}/p53^{-/-}$ counterparts, except for liver, which incorporated significantly less BrdU (Fig. 6C and D). These results suggest that cyclin D-dependent RB phosphorylation is critically required for the proliferation of liver cells but not other cells in the embryo. Another possibility is that the protein levels of cyclin D1 and cyclin D3 are more severely reduced in the fetal liver than in the rest of the mutant embryo. Therefore, we decided to compare the protein expression of D-type cyclins in the liver tissue from E12.5 $S6^{wt/wt}/p53^{-/-}$ and $S6^{wt/del}/p53^{-/-}$ embryos. Cyclin D1 and cyclin D3 were more severely compromised in the $S6^{wt/del}/p53^{-/-}$ liver than in the remaining parts of the embryo (Fig. 6E). These results show that the protein levels of D-type cyclins correlate with the rate of proliferation measured by BrdU incorporation (Fig. 6C and E). However, we do not have direct evidence linking the expression of D-type cyclins and defective fetal liver cell proliferation (Fig. 6E) (23).

At E12.5, the liver is a prominent and externally easily visible organ in $S6^{wt/wt}/p53^{-/-}$ embryos, but it is only marginally evident in $S6^{wt/del}/p53^{-/-}$ embryos (Fig. 7A). Consistent with this observation, E12.5 $S6^{wt/del}/p53^{-/-}$ fetal livers were significantly reduced in size and pale (Fig. 7B).

Impaired fetal liver erythropoiesis and placental defects in $S6^{wt/del}/p53^{-/-}$ embryos. The observed decrease in the proliferation of liver cells in E11.5 $S6^{wt/del}/p53^{-/-}$ embryos (Fig. 6C and D) and the fact that erythropoiesis is a major contributor of liver growth at this stage prompted us to analyze this process (35). H&E staining of liver sections demonstrated severely reduced numbers of immature erythroid cells in $S6^{wt/del}/p53^{-/-}$ embryos (see Fig. S2 in the supplemental material). These results suggest that $S6^{wt/del}/p53^{-/-}$ embryos die as a consequence of diminished definitive erythropoiesis after E12.5. To gain a more precise description of the $S6^{wt/del}/p53^{-/-}$ liver phenotype, we characterized the fetal liver cell population by flow cytometric analysis. For this analysis, we used antibodies against the cell surface markers c-kit and Ter-119. Hematopoietic and erythroid progenitor cells are c-kit positive and Ter-119 negative, whereas proerythroblasts are positive for both cell surface markers. The population that is Ter-119 positive and c-kit negative represents erythroblasts and erythrocytes. The population that is negative for both markers contains hepatocytes and differentiated nonerythroid hematopoietic cells, although the latter are rare at this stage. The percentage of hematopoietic and erythroid progenitor cells (R1) was increased from 10.5% in $S6^{wt/wt}/p53^{-/-}$ livers to 53.7% in $S6^{wt/del}/p53^{-/-}$ livers (Fig. 7C). In contrast, the percentage of erythroblasts and erythrocytes (R3) was reduced from 75% in $S6^{wt/wt}/p53^{-/-}$ livers to 18.3% in $S6^{wt/del}/p53^{-/-}$ livers (Fig. 7C). The percentages of $S6^{wt/del}/p53^{-/-}$ proerythroblast (R2) and hepatocyte (R4) populations in the fetal liver were increased 1.76- and 2.1-fold, respectively (Fig. 7C).

At the E12.5 stage, the total number of cells per liver was decreased from $4.32 \pm 0.85 \times 10^6$ in $S6^{wt/wt}/p53^{-/-}$ ($n = 12$) to

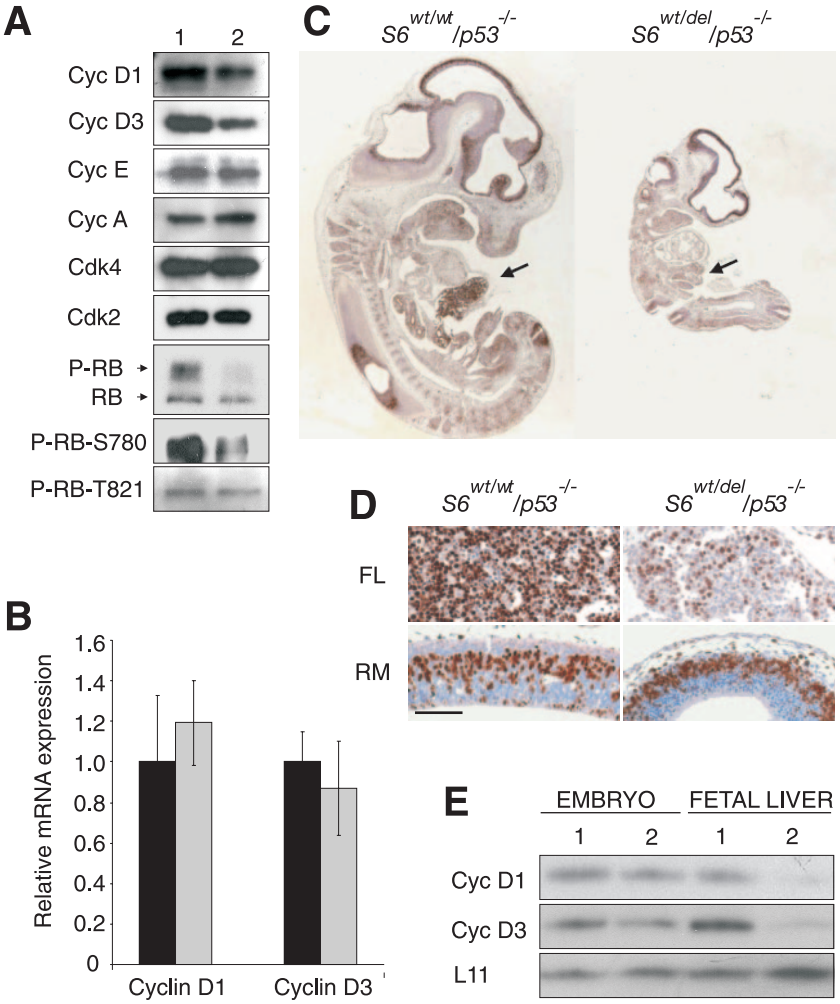

FIG. 6. Characterization of the cell cycle progression in $S6^{wt/del}/p53^{-/-}$ embryos. (A) Western blot analysis of lysates prepared from E10.5 $S6^{wt/wt}/p53^{-/-}$ and $S6^{wt/del}/p53^{-/-}$ embryos using antibodies against the indicated cell cycle regulators. Cyc, cyclin. (B) Quantitative RT-PCR analysis of cyclin D1 and cyclin D3 mRNAs expression in E10.5 $S6^{wt/wt}/p53^{-/-}$ (black bars) and $S6^{wt/del}/p53^{-/-}$ (gray bars) embryos. (C) Sagittal sections of the entire E11.5 embryos of indicated genotypes were stained with anti-BrdU antibody. Fetal livers are indicated by arrows. (D) BrdU incorporation in roofs of midbrain (RM) and fetal livers (FL) of the indicated genotypes (higher magnification of embryo sections from panel E). Scale bar, 100 μm. (E) Lysates of E12.5 fetal livers or the remaining parts of the embryo were analyzed by Western blotting employing antibodies against the indicated proteins. $S6^{wt/wt}/p53^{-/-}$ and $S6^{wt/del}/p53^{-/-}$ genotypes in panels A and E are indicated with 1 and 2, respectively.

$0.48 \pm 0.03 \times 10^6$ in $S6^{wt/wt}/p53^{-/-}$ ($n = 10$) embryos. The compiled results, expressed in terms of the absolute number of cells in each population, showed that there were 1.6- and 3.8-fold decreases in the total number of cells in the R1 and R4 populations, respectively. A 4.7-fold reduction in the number of cells in the R2 population was observed. Strikingly, the R3 population of erythroid differentiating cells was compromised to a much greater degree (31-fold) (Fig. 7D). To analyze this phenotype further, we next plated equal numbers of E12.5 $S6^{wt/wt}/p53^{-/-}$ and $S6^{wt/del}/p53^{-/-}$ fetal liver cells in methylcellulose in the presence of various cytokines and tested the ability of erythroid progenitors to form BFU-E (Fig. 7E). Interestingly, these experiments revealed that the numbers of BFU-E colonies were increased 3.8-fold in the $S6^{wt/del}/p53^{-/-}$ fetal liver cell population relative to the $S6^{wt/wt}/p53^{-/-}$ controls (Fig. 7E), most likely due to a higher representation of c-kit-positive and Ter-119-negative progenitor cells in the mutant fetal liver (R1 population in Fig. 7C). A severely diminished erythropoiesis in E12.5 $S6^{wt/del}/p53^{-/-}$ embryos is likely the result of a modest reduction in the number of erythroid progenitor cells in fetal livers (2.3-fold) (Fig. 7F) and a more severe block in erythropoietic differentiation in vivo (Fig. 7C and D). Interestingly, the size of the colonies formed from individual progenitor cells was indistinguishable between the genotypes (Fig. 7G), suggesting that the intrinsic potential of $S6^{wt/del}/p53^{-/-}$ erythroid progenitors to differentiate in vitro is not significantly altered. The mutant embryos were not obviously anemic, although this is most certainly because of sufficient yolk sac-derived primitive erythropoiesis, which is still active at E12.5 (Fig. 7A and data not shown). Since primitive erythropoiesis ceases after E12.5, there is the possibility that, in the absence of sufficient fetal liver erythropoiesis, $S6^{wt/del}/p53^{-/-}$ embryos die as a result of anemia. Interestingly, mutations in the ribosomal protein *S19* gene are associated with

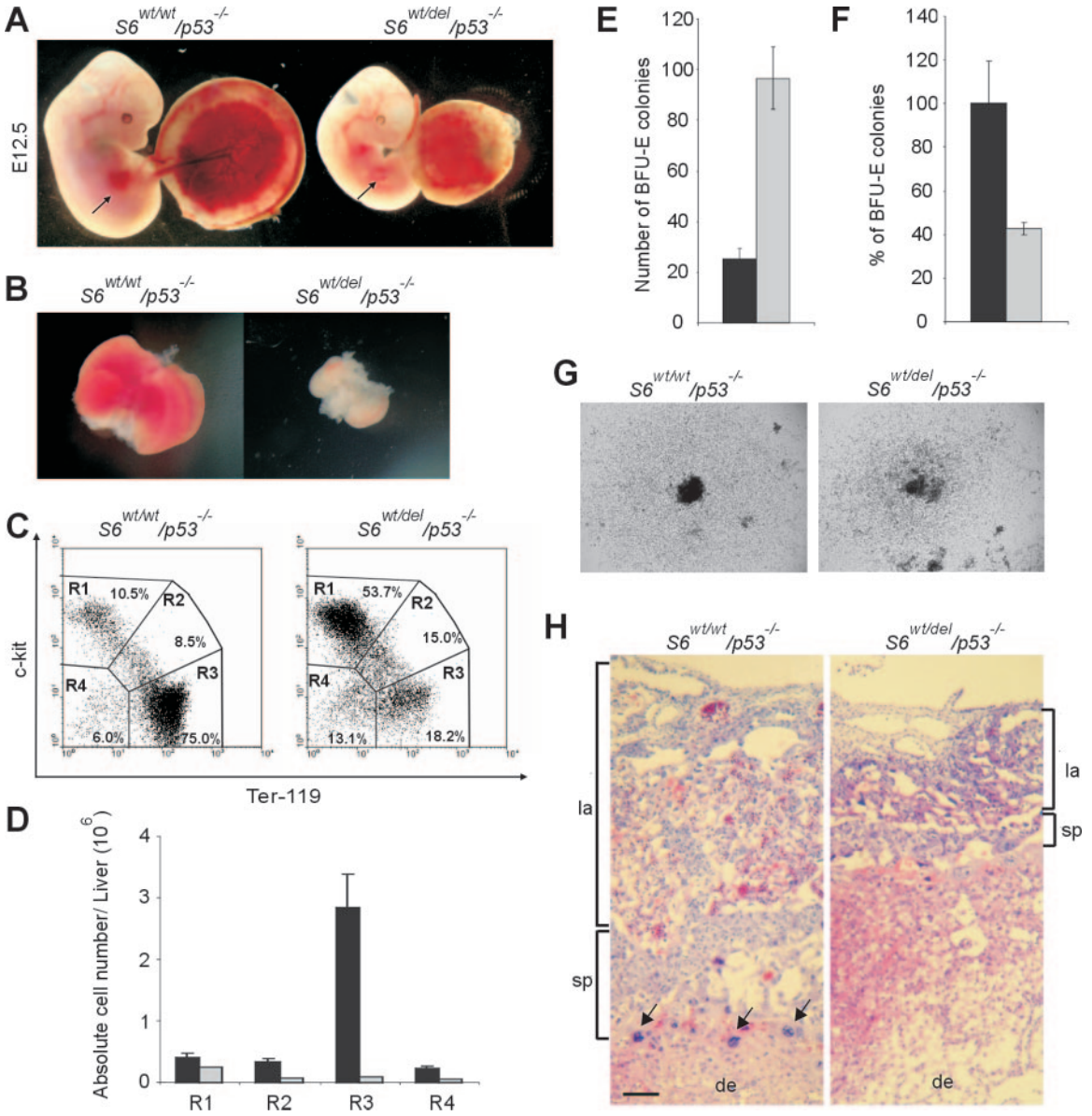

FIG. 7. Impaired fetal liver erythropoiesis and placental defects in $S6^{wt/del}/p53^{-/-}$ embryos. (A) External appearance of representative E12.5 $S6^{wt/wt}/p53^{-/-}$ and $S6^{wt/del}/p53^{-/-}$ littermate embryos together with placentas. Arrows, externally apparent liver in the $S6^{wt/wt}/p53^{-/-}$ embryo and marginally evident liver tissue in the $S6^{wt/del}/p53^{-/-}$ embryo. (B) The picture shows the small size of isolated E12.5 $S6^{wt/del}/p53^{-/-}$ liver compared with the $S6^{wt/wt}/p53^{-/-}$ control. (C) Flow cytometric analysis of the fetal liver cells from E12.5 $S6^{wt/wt}/p53^{-/-}$ and $S6^{wt/del}/p53^{-/-}$ embryos. Cell surface markers are shown as coordinates. Region 1 (R1) includes progenitor cells, R2 includes proerythroblasts, R3 represents erythroblasts and erythrocytes, and R4 includes hepatocytes and potentially other nonerythroid cells. These are representative fluorescence-activated cell sorter profiles. (D) Total numbers of cells in the R1, R2, R3, and R4 populations per fetal liver. The $S6^{wt/wt}/p53^{-/-}$ genotype is shown as black bars and $S6^{wt/del}/p53^{-/-}$ as gray bars. Error bars denote SD. (E) Colony-forming ability of E12.5 $S6^{wt/wt}/p53^{-/-}$ (black bar) and $S6^{wtdel}/p53^{-/-}$ (gray bar) fetal liver hematopoietic progenitors in methylcellulose cultures. Fetal liver cells (2×10^4) were plated in triplicate ($n = 3$ per genotype). Shown are mean numbers of colonies. Error bars indicate SD. The experiment is representative of four independent experiments. (F) Total numbers of BFU-E colonies per fetal liver from E12.5 $S6^{wt/del}/p53^{-/-}$ (gray bar) and $S6^{wt/wt}/p53^{-/-}$ (black bar) embryos. (G) Typical appearance of BFU-E colonies derived from $S6^{wt/wt}/p53^{-/-}$ and $S6^{wt/del}/p53^{-/-}$ samples after 10 days of incubation in methylcellulose culture. Magnification, ×40. (H) H&E staining of histological section of E12.5 $S6^{wt/del}/p53^{-/-}$ placenta shows that the labyrinth (la) and spongiotrophoblast (sp) were significantly reduced relative to the $S6^{wt/wt}/p53^{-/-}$ control. Trophoblast giant cells are indicated by arrows. Decidua (de) is also shown. Scale bar, 100 μm.

some cases of Diamond-Blackfan anemia, which is characterized by absent or decreased erythropoiesis (9).

Morphological examination revealed that the size of $S6^{wt/del}/p53^{-/-}$ placentas was reduced (Fig. 7A). To study placental structure in detail, we performed a histological analysis. H&E staining of a histological section of $S6^{wt/del}/p53^{-/-}$ placenta showed that numbers of labyrinths and spongiotrophoblasts were significantly reduced relative to the $S6^{wt/wt}/$

$p53^{-/-}$ control. Interestingly, the number of trophoblast giant cells was markedly reduced (Fig. 7H). These results suggest that placental defects could be responsible for the lethality of the mutant embryos. Further investigations will be required to determine the exact cause of death of $S6^{wt/del}/p53^{-/-}$ embryos and the contributions of the observed placental phenotype and/or deficient definitive erythropoiesis to the lethality (39).

DISCUSSION

The results presented in this study demonstrate that *S6* gene haploinsufficiency triggers a p53-dependent checkpoint response during gastrulation probably to prevent defective cells from contributing to critical lineages later in development (13). It will be interesting to determine whether this response is the unique feature of the highly proliferating $S6^{wt/del}$ cells in the gastrulating embryo and proliferating T cells or whether it is activated in other cell types as well (44). It has been suggested that nucleolar proteins p19Arf, L5, L11, and L23 are important regulators of p53 levels under stress conditions in vitro (3, 6, 7, 15, 18, 27, 30, 34, 45, 51, 54). It is tempting to speculate that, upon perturbations in ribosome biogenesis in $S6^{wt/del}$ embryonic cells, these proteins participate in p53 activation. The fact that the genetic inactivation of *p19Arf* does not rescue the lethality of *S6*-heterozygous embryos at gastrulation implies that it is not required for this checkpoint response (55). We are currently testing the effect of genetic inactivation of other candidate genes on the phenotype of $S6^{wt/del}$ embryos at gastrulation in vivo. In support of the argument that p53 is being upregulated due to the inhibition of ribosome biogenesis in $S6^{wt/del}$ embryos rather than the ablation of a nonribosomal function of S6 are the observations that other mutations that block ribosome synthesis also trigger the p53 response (37, 52, 56). This issue will be further clarified by comparing the phenotypes of embryos that are heterozygous for other essential ribosomal protein genes with the phenotype of $S6^{wt/del}$ embryos. Many p53 transcriptional targets have been identified as having impacts on the G_1/S and the G_2/M transitions ($p21^{CIP1}$, *GADD45*, *14-3-3*σ, *Cdc25C*, etc.) and apoptosis (*Puma*, *Bax*, and *Noxa*) (47). Since $p21^{CIP1}$ only partially accounts for the effect of p53 to the phenotype (Fig. 3H), it will be necessary to determine the contribution of other candidate genes to the cell cycle block and apoptosis in $S6^{wt/del}$ embryos.

A normal embryonic development of mice whose S6 phosphorylation sites were mutated suggests that a decrease in phospho-S6 does not trigger a checkpoint response (42).

What are the consequences of *S6* heterozygosity on the embryonic development in the absence of p53? Since the translation of specific mRNAs depends on their affinity for ribosome, a defect in ribosome biogenesis in $S6^{wt/del}$ embryos could change the accuracy of protein translation and alter the precise execution of the developmental program (26). Interestingly, despite a defect in ribosome biogenesis, E12.5 $S6^{wt/del}/p53^{-/-}$ MEFs show normal expression of cyclin D1 and D3 proteins, proliferation rates, and sizes. How can these results explain the size difference between $S6^{wt/del}/p53^{-/-}$ and $S6^{wt/wt}/p53^{-/-}$ embryos? We found that the incorporation of BrdU in most tissues of E11.5 $S6^{wt/del}/p53^{-/-}$ embryos was slightly decreased in comparison to their $S6^{wt/wt}/p53^{-/-}$ counterparts, except for liver, which incorporated significantly less BrdU. A slight decrease in BrdU incorporation in $S6^{wt/del}/p53^{-/-}$ relative to $S6^{wt/wt}/p53^{-/-}$ embryos could at least partially account for the size discrepancies between $S6^{wt/del}/p53^{-/-}$ and $S6^{wt/wt}/p53^{-/-}$ embryos. Furthermore, we cannot formally rule out the possibility that a larger defect in proliferation exists in $S6^{wt/del}/p53^{-/-}$ embryos during specific stages of the development. The fact that $S6^{wt/del}/p53^{-/-}$ embryos develop as late as E12.5, when most of the tissues and organs are already formed, indicates that a serious deficiency in the amount of ribosomes in these embryos does not significantly affect the translation of the majority of mRNAs. Indeed, there was no effect on cyclin A, cyclin E, Cdk2, Cdk4, L11, and actin protein levels in these embryos. In contrast, the protein levels of cyclins D1 and D3 were decreased. The observation that the expression of cyclin D1 and D3 mRNAs was normal in $S6^{wt/del}/p53^{-/-}$ embryos suggests a specific defect in their translation. The protein levels of D-type cyclins were more severely compromised within the $S6^{wt/del}/p53^{-/-}$ fetal liver than in the remaining parts of the embryo. These results suggest that decreased levels of D-type cyclins are responsible for the proliferation defect in the mutant fetal liver. However, direct evidence in support of this notion is lacking.

As the progenitors from $S6^{wt/del}/p53^{-/-}$ fetal livers are capable of differentiating along the erythroid lineage in culture, the possibility exists that impaired erythropoiesis in the mutant liver may be secondary to a defect in the other tissues. A feasible candidate tissue that is responsible for the fetal liver phenotype in the mutant embryo may be the placenta, as there are defects in this tissue and placenta has been suggested to influence definitive erythropoiesis in the fetal liver (16). Combining $S6^{wt/del}/p53^{-/-}$ with tetraploid wild-type embryos should help in determining the role of $S6^{wt/del}/p53^{-/-}$ placenta in the mutant fetal liver phenotype and/or the lethality of the embryos (31).

The fact that $S6^{wt/del}/p53^{-/-}$ embryos die at an earlier developmental stage than embryos lacking all D-type cyclins suggests a defective translation of some other mRNAs. It will be challenging to identify them and determine how their translational defects contribute to the phenotype of these embryos. One could also imagine that an uncharacterized p53-independent checkpoint contributes to the phenotype *S6*-heterozygous embryos. These are difficult issues that have to be addressed in the future.

The finding that a p53-dependent checkpoint prevents the development of *S6*-heterozygous embryos during gastrulation, despite the fact that their protein translation is sufficient to allow their development (although aberrant) until E12.5, suggests that the molecular mechanisms have evolved during mammalian evolution; these mechanisms strongly guard against potential heterozygosity for the ribosomal protein *S6* gene and possibly other ribosomal protein genes. Since some ribosomal protein genes are suggested to be tumor suppressors (1, 9, 50), we speculate that the failure to activate a p53-dependent checkpoint when an error in ribosome biogenesis or defective ribosomes are present could potentially lead to the development of malignant tumors (32). Additionally, the activation of this checkpoint might

play an important role in development, senescence, and aging.

ACKNOWLEDGMENTS

We are grateful to George Thomas and Sara Kozma for their continuous support of our work; Jacques Montagne, Jonathan Ashwell, Nick Pullen, Ivan Đikić, and Stefano Fumagalli for readings of the manuscript; Drago Batinić and Tihomila Bušić for technical advice; and Barbara Knowles and Charles Sherr for providing *Zp3-Cre* transgenic mice and *p19Arf* knockout mice, respectively.

This work was supported by grants from SNSF and the Ministry of Science, Education, and Sports of Croatia.

REFERENCES

1. **Amsterdam, A., K. C. Sadler, K. Lai, S. Farrington, R. T. Bronson, J. A. Lees, and N. Hopkins.** 2004. Many ribosomal protein genes are cancer genes in zebrafish. PloS Biol. **2:**E139.
2. **Bartkova, J., Z. Horejsi, K. Koed, A. Kramer, F. Tort, K. Zieger, P. Guldberg, M. Sehested, J. M. Nesland, C. Lukas, T. Orntoft, J. Lukas, and J. Bartek.** 2005. DNA damage response as a candidate anti-cancer barrier in early human tumorigenesis. Nature **434:**864–870.
3. **Bhat, K. P., K. Itahana, A. Jin, and Y. Zhang.** 2004. Essential role for ribosomal protein L11 in mediating growth inhibition-induced p53 activation. EMBO J. **23:**2402–2412.
4. **Brugarolas, J., C. Chandrasekaran, J. I. Gordon, D. Beach, T. Jacks, and G. J. Hannon.** 1995. Radiation-induced cell cycle arrest compromised by p21 deficiency. Nature **377:**552–557.
5. **Conlon, I., and M. Raff.** 1999. Size control in animal development. Cell **96:**235–244.
6. **Dai, M. S., and H. Lu.** 2004. Inhibition of MDM2-mediated p53 ubiquitination and degradation by ribosomal protein L5. J. Biol. Chem. **279:**44475–44482.
7. **Dai, M. S., S. X. Zeng, Y. Jin, X. X. Sun, L. David, and H. Lu.** 2004. Ribosomal protein L23 activates p53 by inhibiting MDM2 function in response to ribosomal perturbation but not to translation inhibition. Mol. Cell. Biol. **24:**7654–7668.
8. **de Vries, W. N., L. T. Binns, K. S. Fancher, J. Dean, R. Moore, R. Kemler, and B. B. Knowles.** 2000. Expression of Cre recombinase in mouse oocytes: a means to study maternal effect genes. Genesis **26:**110–112.
9. **Draptchinskaia, N., P. Gustavsson, B. Andersson, M. Pettersson, T. N. Willig, I. Dianzani, S. Ball, G. Tchernia, J. Klar, H. Matsson, D. Tentler, N. Mohandas, B. Carlsson, and N. Dahl.** 1999. The gene encoding ribosomal protein S19 is mutated in Diamond-Blackfan anaemia. Nat. Genet. **21:**169–175.
10. **Elledge, S. J.** 1996. Cell cycle checkpoints: preventing an identity crisis. Science **274:**1664–1672.
11. **Hafen, E.** 2004. Interplay between growth factor and nutrient signaling: lessons from *Drosophila* TOR. Curr. Top. Microbiol. Immunol. **279:**153–167.
12. **Hayashi, S., P. Lewis, L. Pevny, and A. P. McMahon.** 2002. Efficient gene modulation in mouse epiblast using a *Sox2Cre* transgenic mouse strain. Mech. Dev. **119**(Suppl. 1)**:**S97–S101.
13. **Heyer, B. S., A. MacAuley, O. Behrendtsen, and Z. Werb.** 2000. Hypersensitivity to DNA damage leads to increased apoptosis during early mouse development. Genes Dev. **14:**2072–2084.
14. **Holland, E. J., N. Sonenberg, P. P. Pandolfi, and G. Thomas.** 2004. Signaling control of mRNA translation in cancer pathogenesis. Oncogene **23:**3138–3144.
15. **Honda, R., and H. Yasuda.** 1999. Association of $p19^{ARF}$ with Mdm2 inhibits ubiquitin ligase activity of Mdm2 for tumor suppressor p53. EMBO J. **18:**22–27.
16. **Ihle, J. N.** 2000. The challenges of translating knockout phenotypes into gene function. Cell **102:**131–134.
17. **Jacks, T., L. Remington, B. O. Williams, E. M. Schmitt, S. Halachmi, R. T. Bronson, and R. A. Weinberg.** 1994. Tumor spectrum analysis in p53-mutant mice. Curr. Biol. **4:**1–7.
18. **Jin, A., K. Itahana, K. O'Keefe, and Y. Zhang.** 2004. Inhibition of HDM2 and activation of p53 by ribosomal protein L23. Mol. Cell. Biol. **24:**7669–7680.
19. **Jorgensen, P., J. L. Nishikawa, B. J. Breitkreutz, and M. Tyers.** 2002. Systematic identification of pathways that couple cell growth and division in yeast. Science **297:**395–400.
20. **Jorgensen, P., and M. Tyers.** 2004. How cells coordinate growth and division. Curr. Biol. **14:**R1014–1027.
21. **Kastan, M. B., and J. Bartek.** 2004. Cell-cycle checkpoints and cancer. Nature **432:**316–323.
22. **Kopecny, V., V. Landa, and A. Pavlok.** 1995. Localization of nucleic acids in the nucleoli of oocytes and early embryos of mouse and hamster: an autoradiographic study. Mol. Reprod. Dev. **41:**449–458.
23. **Kozar, K., M. A. Ciemerych, V. I. Rebel, H. Shigematsu, A. Zagozdzon, E. Sicinska, Y. Geng, Q. Yu, S. Bhattacharya, R. T. Bronson, K. Akashi, and P. Sicinski.** 2004. Mouse development and cell proliferation in the absence of D-cyclins. Cell **118:**477–491.
24. **LaMarca, M. J., and P. M. Wassarman.** 1979. Program of early development in the mammal: changes in absolute rates of synthesis of ribosomal proteins during oogenesis and early embryogenesis in the mouse. Dev. Biol. **71:**103–119.
25. **Lambertsson, A.** 1998. The minute genes in *Drosophila* and their molecular functions. Adv. Genet. **38:**69–134.
26. **Lodish, H. F.** 1974. Model for the regulation of mRNA translation applied to haemoglobin synthesis. Nature **251:**385–388.
27. **Lohrum, M. A., R. L. Ludwig, M. H. Kubbutat, M. Hanlon, and K. H. Vousden.** 2003. Regulation of HDM2 activity by the ribosomal protein L11. Cancer Cell **3:**577–587.
28. **Lowe, S. W., and C. J. Sherr.** 2003. Tumor suppression by *Ink4a-Arf*: progress and puzzles. Curr. Opin. Genet. Dev. **13:**77–83.
29. **Lyons, A. B., and C. R. Parish.** 1994. Determination of lymphocyte division by flow cytometry. J. Immunol. Methods **171:**131–137.
30. **Marechal, V., B. Elenbaas, J. Piette, J. C. Nicolas, and A. J. Levine.** 1994. The ribosomal protein L5 protein is associated with Mdm-2 and Mdm-2–p53 complexes. Mol. Cell. Biol. **14:**7414–7420.
31. **Nagy, A., M. Gertsenstein, K. Vintersten, and R. Behringer.** 2003. Manipulating the mouse embryo: a laboratory manual, 3rd ed. Cold Spring Harbor Laboratory Press, Cold Spring Harbor, N.Y.
32. **Nurse, P.** 2000. A long twentieth century of the cell cycle and beyond. Cell **100:**71–78.
33. **O'Farrell, P. H., J. Stumpff, and T. T. Su.** 2004. Embryonic cleavage cycles: how is a mouse like a fly? Curr. Biol. **14:**R35–45.
34. **Olson, M. O. J.** 2004. Sensing cellular stress: another new function for the nucleolus? Sci. STKE **224:**pe10.
35. **Palis, J., S. Robertson, M. Kennedy, C. Wall, and G. Keller.** 1999. Development of erythroid and myeloid progenitors in the yolk sac and embryo proper of the mouse. Development **126:**5073–5084.
36. **Pardee, A. B.** 1989. G_1 events and regulation of cell proliferation. Science **246:**603–608.
37. **Pestov, D. G., Z. Strezoska, and L. F. Lau.** 2001. Evidence of p53-dependent cross-talk between ribosome biogenesis and the cell cycle: effects of nucleolar protein Bop1 on G_1/S transition. Mol. Cell. Biol. **21:**4246–4255.
38. **Rathmell, J. C., M. G. Vander Heiden, M. H. Harris, K. A. Frauwirth, and C. B. Thompson.** 2000. In the absence of extrinsic signals, nutrient utilisation by lymphocytes is insufficient to maintain either cell size or viability. Mol. Cell **6:**683–692.
39. **Rossant, J., and J. C. Cross.** 2001. Placental development: lessons from mouse mutants. Nat. Rev. Genet. **2:**538–548.
40. **Rudra, D., and J. R. Warner.** 2004. What better measure than ribosome synthesis? Genes Dev. **18:**2431–2436.
41. **Ruggero, D., and P. P. Pandolfi.** 2003. Does the ribosome translate cancer? Nat. Rev. Cancer **3:**179–192.
42. **Ruvinsky, I., N. Sharon, T. Lerer, H. Cohen, M. Stolovich-Rain, T. Nir, Y. Dor, P. Zisman, and O. Meyuhas.** 2005. Ribosomal protein S6 phosphorylation is a determinant of cell size and glucose homeostasis. Genes Dev. **19:**2199–2211.
43. **Schmelzle, T., and M. N. Hall.** 2000. TOR, a central controller of cell growth. Cell **103:**253–262.
44. **Šulić, S., L. Panić, M. Barkić, M. Merćep, M. Uzelac, and S. Volarević.** 2005. Inactivation of S6 ribosomal protein gene in T lymphocytes activates a p53-dependent checkpoint response. Genes Dev. **19:**3070–3082.
45. **Tao, W., and A. J. Levine.** 1999. $p19^{ARF}$ stabilizes p53 by blocking nucleocytoplasmic shuttling of Mdm2. Proc. Natl. Acad. Sci. USA. **96:**6937–6941.
46. **Thomas, G.** 2000. An encore for ribosome biogenesis in cell proliferation. Nat. Cell Biol. **2:**E71–E72.
47. **Vogelstein, B., D. Lane, and A. J. Levine.** 2000. Surfing the p53 network. Nature **408:**307–310.
48. **Volarević, S., M. J. Stewart, B. Ledermann, F. Zilberman, L. Terracciano, E. Montini, M. Grompe, S. C. Kozma, and G. Thomas.** 2000. Cell proliferation blocked by conditional deletion of 40S ribosomal protein S6. Science **288:**2045–2047.
49. **Volarević, S., and G. Thomas.** 2001. Role of S6 phosphorylation and S6 kinase in cell growth. Prog. Nucleic. Acids Res. Mol. Biol. **65:**101–127.
50. **Watson, K. L., K. D. Konrad, D. F. Woods, and P. J. Bryat.** 1992. *Drosophila* homolog of the human S6 ribosomal protein is required for tumor suppression in the hematopoietic system. Proc. Natl. Acad. Sci. USA **89:**11302–11306.
51. **Weber, J. D., M. L. Kuo, B. Bothner, E. L. DiGiammarino, R. W. Kriwacki, M. F. Roussel, and C. J. Sherr.** 2000. Cooperative signals governing ARF-Mdm2 interaction and nucleolar localization of the complex. Mol. Cell. Biol. **20:**2517–2528.
52. **Wool, I. G.** 1996. Extraribosomal functions of ribosomal proteins. Trends Biochem. Sci. **21:**164–165.
53. **Zhang, J., C. Schneider, L. Ottmers, R. Rodriguez, A. Day, J. Markwardt, and B. L. Schneider.** 2002. Genomic scale mutant hunt identifies cell size homeostasis genes in *Saccharomyces cerevisiae*. Curr. Biol. **12:**1992–2001.

54. **Zhang, Y., G. W. Wolf, K. Bhat, A. Jin, T. Allio, W. A. Burkhart, and Y. Xiong.** 2003. Ribosomal protein L11 negatively regulates oncoprotein MDM2 and mediates a p53-dependent ribosomal-stress checkpoint pathway. Mol. Cell. Biol. **23:**8902–8912.
55. **Zindy, F., R. T. Williams, J. E. Rehg, S. X. Skapek, J. L. Cleveland, M. F. Roussel, and C. J. Sherr.** 2003. Arf tumor suppressor promoter monitors latent oncogenic signals in vivo. Proc. Natl. Acad. Sci. USA **100:**15930–15935.
56. **Yuan, X., Y. Zhou, E. Casanova, M. Chai, E. Kiss, H. J. Grone, G. Schutz, and I. Grummt.** 2005. Genetic inactivation of the transcription factor TIF-IA leads to nucleolar disruption, cell cycle arrest, and p53-mediated apoptosis. Mol. Cell **19:**77–87.